Progress and prospective of heterogeneous catalysts for H_2O_2 production via anthraquinone process

Anjali A. Ingle[1] [iD] · Shahid Z. Ansari[2] · Diwakar Z. Shende[1] [iD] · Kailas L. Wasewar[1] [iD] · Aniruddha B. Pandit[2]

Abstract

This paper reviews the improvement in the field of catalytic hydrogenation of 2-ethylanthraquinone to 2-ethylanthrahydroquinone for the successful production of hydrogen peroxide. Hydrogen peroxide is being used in almost all industrial areas, particularly in the chemical industry and in environmental protection, as the most promising oxidant for cleaner and environmentally safer processes. A variety of hydrogenation catalysts have been introduced for hydrogenation of 2-ethylanthraquinone in the production of hydrogen peroxide via anthraquinone (AQ) process. The aim of the present study is to describe the catalysts used in the hydrogenation of 2-ethylanthraquinone and the reaction mechanism involved with different catalytic systems. The hydrogenation of 2-ethylanthraquinone using metals, alloy, bimetallic composite, and supported metal catalyst with the structural modifications has been incorporated for the production of hydrogen peroxide. The comprehensive comparison reveals that the supported metal catalysts required lesser catalyst amount, produced lower AQ decay, and provided higher catalyst activity and selectivity. Furthermore, the replacement of conventional catalysts by metal and metal alloy–supported catalyst rises as a hydrogenation trend, enhancing by several times the catalytic performance.

Keywords Hydrogen peroxide · Anthraquinone process · Heterogeneous catalyst · Reaction mechanism

Introduction

Thenard, a French chemist, discovered hydrogen peroxide (H_2O_2) in 1818 (Chalmers 1996). The industrial manufacturing of H_2O_2 was introduced by reacting barium peroxide (BaO_2) with sulfuric acid, hydrochloric acid, and phosphoric acid in late 1885 (Van 1968). The demand for H_2O_2 is increasing constantly because of its favorable oxidation properties. It is an essential raw material for industrial green chemicals and environmentally friendly oxidizing agents (Jose et al. 2006; Yao et al., 2016a; Gema et al. 2016; Han et al., 2015a; Tan et al. 2012; Melada et al. 2006; Garcia-Serna et al., 2014). H_2O_2 is being used in various grades in the food storage and cosmetic and electronic industries. In the recent COVID-19 era, demand of healthcare products is increasing as H_2O_2 has high antiseptic properties which directly boost its market value. H_2O_2 is used as an antiseptic, which is commonly applied on the skin cuts and bruises to avoid infection. Furthermore, in light of the recent COVID-19 pandemic, demand for H_2O_2 has grown significantly worldwide due to its high consumption in the formulation of disinfectant products. H_2O_2 is the main ingredients in hand sanitizers whose demand has increased simultaneously all over the world.

The H_2O_2 has been used in the textile, food, mining, pulp, and paper industries and for the wastewater treatment. It is also used in the manufacture of printed circuit boards for semiconductors and also has good demand in aquaculture

✉ Diwakar Z. Shende
diwakar.shende@gmail.com

Anjali A. Ingle
anjuingle2013@gmail.com

Shahid Z. Ansari
shahidtechno.87@gmail.com

Kailas L. Wasewar
k_wasewar@rediffmail.com

Aniruddha B. Pandit
ab.pandit@ictmumbai.edu.in

[1] Advanced Separation and Analytical Laboratory (ASAL), Department of Chemical Engineering, Visvesvaraya National Institute of Technology, Nagpur, Maharashtra 440010, India

[2] Department of Chemical Engineering, Institute of Chemical Technology (ICT), Mumbai, Maharashtra 400019, India

market (Jose et al. 2006; Rosaria et al. 2016). The average plant capacity of H_2O_2 production was 20–40 kT per year with a world capacity of 1.5 million tons up to mid of 1990 (Ranganathan and Sieber, 2018). The plant capacity increases to 300 kT per year with a world capacity of 100% H_2O_2 which is around 5.5 million tons in 2015 (Ciriminna et al. 2016; Ranganathan and Sieber, 2018). The global producers of H_2O_2 involves Solvay (30%), Evonik (20%), and Arkema (13%) (Garcia-Serna et al. 2014).

Production of hydrogen peroxide

Autoxidation (AO) of anthraquinone (AQ), oxidation of primary and secondary alcohols, and electrochemical process are the commercial processes for the production of H_2O_2 (Foller and Bombard, 1995). The direct introduction of

Fig. 1 A typical production route of hydrogen peroxide

hydrogen (H_2) and oxygen (O_2) over hydrogenation catalyst (Chen et al. 2013) semiconductor oxide photocatalytic reactions (Gabriele et al. 2003) and the incorporation of metal complexes in $CO/O_2/H_2O$ mixture (Zudin et al. 1979) are the new synthesis processes for the production of H_2O_2. The different routes of the production of H_2O_2 are depicted in Fig. 1. However, the abovementioned processes carry the high risk of explosion and also suffer from low concentration of H_2O_2. Due to larger production scale and high concentration of H_2O_2, the AQ process overcomes the flaws of high energy consumption and larger production cost and surpasses all commercial processes with mild reaction temperatures and lower production costs. The conventional AQ process involved the sequential hydrogenation of an AQ derivative, mainly 2-ethylanthraquinone (EAQ), and the oxidation of 2-ethylanthrahydroquinone ($EAQH_2$). The world production of H_2O_2 is dominated by the AQ process in which EAQ is dissolved in a mixture of polar and nonpolar solvents. The resulting working solution is hydrogenated to $EAQH_2$ in the presence of hydrogenation catalysts. $EAQH_2$ is then converted to H_2O_2 and EAQ after oxidation. A simplified production route of this AQ process is shown in Fig. 2. H_2O_2 is miscible with water in all proportions; hence, it can be recovered in extract phase by multiple washing of organic phase and enhances the concentration up to 50% by distillation process (Liu et al. 2005; Cheng et al. 2008). The overall world share of H_2O_2 production by the AQ process is about 98% (Guo et al. 2019).

The hydrogenation of EAQ in the presence of a catalyst is the key step in the production of H_2O_2 via the AQ process. I. G. Farbenindustries (1939) investigated the first commercial process in Germany for hydrogenation of EAQ in which $EAQH_2$ was formed in a slurry reactor over a Pd/Al_2O_3 catalyst (Goor et al. 1989; Kirchner 1979). The working solution was a combination of two organic solvents, namely benzene and a mixture of secondary alcohols (C7–C11). The concentration of the H_2O_2 solution obtained from the AQ process was about 0.6–1.8 wt%. It is important to enhance the efficiency of the AQ process by improving the purity of the
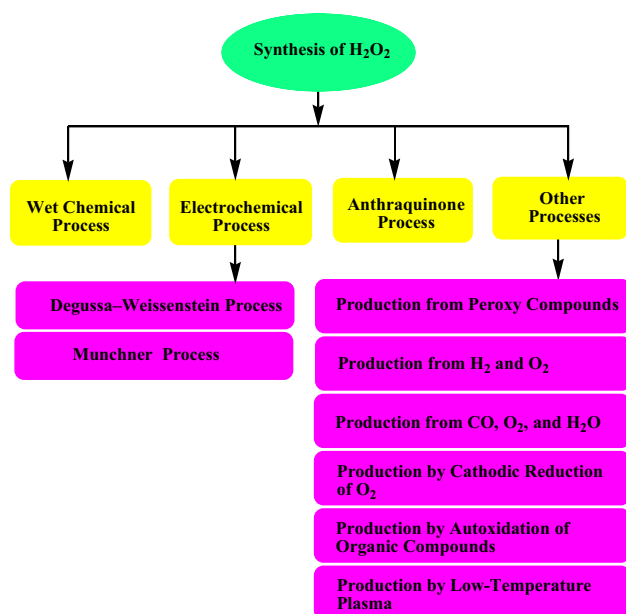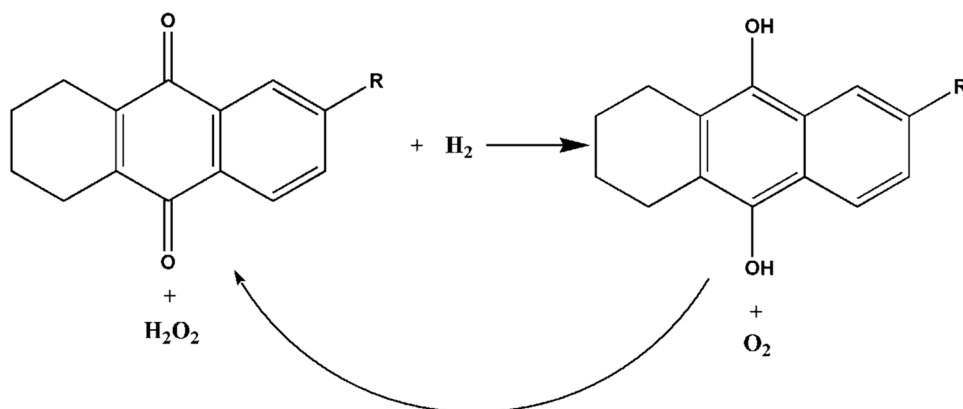
Fig. 2 A simplified production route by the AQ process

resulting H_2O_2 solution (Ren et al. 2011). Tang et al. (2014) describe the importance of catalyst support to enhance the diffusion rate as well as the dispersion of active metals. The spherical alumina has been used widely in the fixed bed reactor as catalyst support due to its excellent physical and chemical properties. Li et al. (2012) invented the Pd supported on whisker-modified spherical alumina, resulting in better catalytic activity than the convention pelleted catalyst.

This study is a review-based finding of different researchers, predominating on the hydrogenation of EAQ using Pd-supported catalysts. The focus is given on the progress in the research and development of the catalytic hydrogenation of EAQ for the production of H_2O_2 by the AQ process. The study discusses primarily the development in the field of new hydrogenation catalysts mainly oxide-supported catalysts for the AQ process. Furthermore, the preparation of Pd catalysts supported on Al_2O_3, SiO_2, and other novel catalyst systems was performed with an attempt to possibly elaborate the significant improvement in the literature. Thus, the present paper describes the advances in the preparation of Pd catalysts on various oxide supports and also other advanced catalysts with structured supports and summarized the general outlook of the developments in the associated area.

Role of oxidizing agent

An oxidizing agent (often referred to as an oxidizer or an oxidant) is a chemical species that tends to oxidize other substances, i.e., causing an increase in the oxidation state of the substance by making it lose electrons. Common examples of oxidizing agents include halogens (such as chlorine and fluorine), O_2, and H_2O_2.

Consumption of H_2O_2 is increasing day by day in the current forecast period and gaining importance as an environmentally friendly and efficient disinfecting agent because of the increased environmental awareness globally and more stringent legislative requirements. It can be added to the coloring liquid for efficient bleaching operation in the textile industry (Asghar et al. 2015; Karmakar 1999). It has been mixed with the reaction mixture to accelerate the oxidation reaction in an organosynthesis process for the production of fine and bulk chemicals (Sato et al. 1998). It is a promising substitute as an energy carrier used in the production of fuel cells because of its high density, safe handling, and easy storage (Yamazaki et al. 2008; Shaegh et al. 2012; Yamada et al. 2013; Yang et al. 2013). It can be united with a light source, catalyst, and ozone to remove various gaseous and aqueous pollutants from the effluent treatment plant. H_2O_2 is generally used in the wastewater treatment plant for wet peroxide oxidation, Fenton and photo-Fenton oxidations, sono-Fenton, electro-Fenton, and photocatalytic degradation reactions (Vieira et al. 2022; Perathoner and Centi, 2005;

Rokhina and Virkutyte, 2010; Debellefontaine et al. 1996; Domingues et al. 2017; Gomes et al. 2010; Ribeiro et al. 2013, 2016, 2015). In situ generation of H_2O_2 or may be combining it with the photocatalytic water treatment process enhances the degradation of pollutants due to its promoting effect (Cui et al. 2012; Yao et al. 2016b; Kumar et al. 2017; Zhou et al. 2018; Deng et al. 2017).

In municipal wastewater treatment, H_2O_2 is used to remove hydrogen sulfide (H_2S) from the sewer pipes. It is mostly significantly used in an environmental application for the treatment of various types of industrial wastes. The H_2O_2 treatment can easily remove the cyanide, thiocyanate, nitrite, chloride, hypochlorite, and organic matter (Chidambara Raj and Quen, 2005). It can also be used in an advanced oxidation process involving more complex reactions as a source of hydroxyl radicals (Chidambara Raj and Quen, 2005; Vieira et al. 2020a, 2020b). H_2O_2 is used in the bulk sludge biological treatment as a source of oxygen and to prevent denitrification in the settling tanks. H_2O_2 can also be combined in the injection as a source of oxygen for microorganisms and nutrients to inject into the ground for in situ bioremediation of contaminated soils. H_2O_2 can be employed in the manufacturing of many organic and inorganic chemicals either directly or followed by conversion into a peroxycarboxylic acid using oxidation, epoxidation, hydroxylation, and oxohalogenation reactions, and for the initiation of emulsion polymerization reactions to produce chemicals like hydrazine, cyanogen, cyanogen chloride, bromine, iodic acid, high-purity ferric sulfate, perborates, percarbonates, benzyl peroxide, and lauryl peroxide (Centi et al. 2009; Bremner et al. 2000; Niwa et al. 2002; Jiajian et al. 2003; Ligtenbarg et al. 2003; Immanuel et al. 2003).

H_2O_2 can be used in a variety of applications in the mining and metal processing industry (Jennings et al. 2000). The major applications of H_2O_2 in the mining operations consist of extraction, separation, and purification of uranium, chromium, copper, cobalt, tungsten, molybdenum, gold recovery, and other precious metals. H_2O_2 can also be used in the metal finishing process for etching, stainless steel pickling, and non-ferrous metal finishing. High-purity H_2O_2 is used in the electronic industry for cleaning germanium and silicon semiconductor wafers and etching printed circuit boards. In chemical and pharmaceutical syntheses, hydrocarbons, nitrogen oxides, and sulfur dioxide in H_2S coming from the exhaust gases can be removed by H_2O_2 (Jose et al. 2006).

Hydrogenation of 2-ethylanthraquinone

The hydrogenation of EAQ has been studied extensively using various kinds of catalyst. However, the modified Pd-based catalysts are the significant catalytic system. Therefore, the improvements in the existing structure of the

catalysts are the important point of consideration for the process development (Liu et al. 2005; Cheng et al. 2008; Li et al. 2012; Isaka et al. 2016; Freakley et al. 2016; Hong et al. 2015; Kosydar et al. 2011; Drelinkiewicz et al., 2005, 2006a, b). In the conventional AQ process, Rn-Ni catalysts have been used in the hydrogenation of EAQ. Rn-Ni catalysts have been replaced by Pd-supported catalysts in the industry due to its higher catalytic activity and selectivity of active quinone observed in the hydrogenation reactions (Liu et al. 2001; Hou et al. 2004). The supported catalysts provide better catalytic activity due to a more effective surface area available with smaller catalyst particles and the higher active metal component dispersion. They are thermally stable and can undergo high temperature and carry higher specific surface area (Hermans and Geus, 1979). The Pd metal on various supports has been used in the hydrogenation of EAQ in both batch and continuous processes.

The supported catalysts are gaining recognition in the field of catalysis due to their superior catalytic performance. Zhang and co-workers (2017) proposed the hydrogenation of EAQ in presence of the bimetallic Pd-Ru catalyst on γ-alumina. Yuan et al. (2017) investigated the effects of synergistic forces due to the addition of second metal such as Co, Ag, and Cu to the conventional catalyst Pd/Al$_2$O$_3$ in the hydrogenation of EAQ. The performance of the supported catalysts has been enhanced due to the size, crystal facet, and electronic structure of Pd particles. Li and Luo enhanced the supports by alternate modification using various methods of preparations to increase the dispersion of metal for higher catalyst activity and selectivity (Tang et al. 2014; Li et al. 2012; Feng et al. 2010; Liu et al. 2002).

In the previous studies, the catalytic hydrogenation of EAQ has been done using the monometallic (Ni, Pd, Ag, Cu) and the bimetallic (Pd-Co, Pd-Ag, Pd-Cu) catalysts. The Ni-B catalysts have been used in the hydrogenation of EAQ, and the results show the influence of the support structure on the catalytic activity and selectivity (Liu et al. 2001, 2002). Ni-Al and Ni-Cr-B-supported catalysts have also been used in the hydrogenation of EAQ. Han et al. (2015a) focused on the modification of supports with the facet-controlled Pd nanocrystals in the hydrogenation of EAQ. A specific method to enhance the catalytic performance of Pd nanocrystals is to place specific highly active facets instead of single-crystal nanoparticles (Jin et al. 2012). Drelinkiewicz and Hasik (2001) and Kosydar et al. (2010) studied extensively to lead the high-performance catalyst for hydrogenation reaction. It was found that the modification in the existing Al$_2$O$_3$ or SiO$_2$ support to enhance the adsorption properties may retard the rate of reaction in the "deep hydrogenation" stage due to the addition of Na$_2$SiO$_3$, polyaniline, or alkali metals such as Li, Na, K, and Cs (Kosydar et al. 2010, 2011; Drelinkiewicz and Hasik 2001; Drelinkiewicz et al., 2004a, b, 2005, 2007; Drelinkiewicz

and Waksmundzka-Gora, 2006a, b). It was also investigated that the dispersion of Pd metal enhances with a decrease in the diffusion resistance due to the modification in the pore structure of the support. Han et al. (2015a) have focused on the modification of supports with preparing the high-performance catalysts by enhancing the catalytic chemistry of the Pd-based catalysts.

Pd/γ-Al$_2$O$_3$ catalyst was synthesized by Chen et al. (2015) by plant-mediated strategy for hydrogenation of EAQ with the adsorption-reduction method. Pd-Au/Al$_2$O$_3$ catalyst with special structural and electronic properties shows better catalytic performance in the hydrogenation reaction of EAQ (Han et al., 2015b). A combination of impregnation (IM) and deposition-precipitation (DP) methods was incorporated for the preparation of the bimetallic Pd-Au/Al$_2$O$_3$ catalyst with higher performance for the hydrogenation reaction of EAQ. The mass transfer–controlled hydrogenation of EAQ in the presence of the Pd catalyst was carried out by Santacesaria et al. (1994a, b), and they observed it as a very fast reaction. The hydrogenation of EAQ was confirmed to be zero- and first-order kinetic with respect to hydrogen and EAQ concentrations, respectively (Shang et al. 2012; Santacesaria et al. 1999, 1988; Berglin and Schoon, 1981). The glass beads with an eggshell structure have been used to support Pd nanoparticles and found to be a new catalyst in the hydrogenation of EAQ. Na$_2$SiO$_3$ and MgSiO$_3$ contents in glass beads resulted in its alkalinity, and hence, the glass beads with porous eggshell structure are well suited to combine with the Pd nanoparticles (Shen et al. 2011; Sun et al. 2008a, 2008b).

Catalytic performance and reaction mechanism

The supported catalysts for EAQ hydrogenation can be classified into three categories: (1) Al$_2$O$_3$-supported catalysts, comprised of noble metal Pd and bimetallic Pd (Pd-Ru, Pd-Au, and Pd-Ag) catalysts supported on Al$_2$O$_3$; (2) SiO$_2$-supported catalysts; and (3) catalysts with advanced structure such as Al$_2$O$_3$-SiO$_2$, ZrO$_2$-γ-Al$_2$O$_3$, glass beads, functionalized SBA-15, and honeycomb cordierite monolith catalysts.

Al$_2$O$_3$-supported Pd catalysts

An extensive study on the investigations of hydrogenation catalysts with experimental runs and theoretical discussions was attempted in the past (Han et al. 2015a; Tang et al. 2014; Li et al. 2012; Drelinkiewicz et al. 2005; Shi et al. 2016). Although the various metal-based catalysts were used in the production of H$_2$O$_2$ by different methods, the Pd-supported catalysts provide a better hydrogenation effect among all

catalysts. The various Pd catalysts supported on Al$_2$O$_3$ are presented in Table 1. Ulmann (1994) mentioned the H$_2$O$_2$ is produced by mixing 30% EAQ, 70% 2-ethyl-tetrahydroanthraquinone (THEAQ), and organic solvents followed by hydrogenation and oxidation as depicted in Fig. 3. The kinetic of hydrogenation of EAQ can be affected by internal diffusion mass transfer limitation because of a very fast reaction occurring over the Pd catalyst in a semi-batch reactor. Hence, they studied the kinetic for hydrogenation reaction measuring in terms of hydrogen consumption and rotating speed. It can be observed that the kinetics follow a zero-order kinetic for hydrogen and a first-order kinetic for THEAQ. Thus, the kinetics confirm that the THEAQ hydrogenation follows the Rideal-Eley mechanism. The hydrogenation reaction over the Pd catalyst has great affinity; hence, dissociative adsorption of hydrogen on the Pd catalyst is very high (Santacesaria et al. 1988).

The necessity to add a fresh catalyst in the industrial reactor to enhance productivity is a relevant consequence due to catalyst poisoning. Here, two types of catalyst poisoning were observed: reversible poisoning with water molecules adsorbed on Pd catalytic sites and irreversible poisoning

Table 1 Hydrogenation of EAQ using various Pd-supported catalysts

Catalyst	Process conditions	Synthesis methods	References
Pd/Al$_2$O$_3$	0.1 MPa, 70 °C	Impregnation	Santacesaria et al. (1999)
Pd/γ-Al$_2$O$_3$	0.3 MPa, 40 °C	Adsorption-reduction	Chen et al. (2015)
Pd/Al$_2$O$_3$	0.3 MPa, 45 °C	Polyol method	Li et al. (2016a)
Pd Al$_2$O$_3$	0.3 MPa, 70 °C	EISA, HT, impregnation	Yuan et al. (2016)
Pd-Ru/γ-Al$_2$O$_3$	0.3 MPa, 60 °C	Facile incipient wetness impregnation	Zhang et al. (2017)
Pd/γ-Al$_2$O$_3$	0.2 MPa, 50 °C	1-step synthesis	Han et al. (2015a)
Pd-Au/Al$_2$O$_3$	0.3 MPa, 60 °C	Deposition-impregnation	Han et al. (2015b)
Pd/δ-Al$_2$O$_3$	0.1 MPa, 50 °C	Oil column	Li et al. (2012)
Pd/AAO@Al	0.1 MPa, 50 °C	2-step low-potential anodizing/impregnation	Hong et al. (2015)
Pd/SiO$_2$	0.1 MPa, 21 °C	Dry impregnation	Drelinkiewicz (1992)
Pd/SiO$_2$	0.5 MPa, 50 °C	Impregnation, precipitation	Drelinkiewicz et al. (2004a)
Pd/Al$_2$O$_3$	0.3 MPa, 70 °C	Incipient wetness co-impregnation	Yuan et al. (2017)
Pd/Al$_2$O$_3$	0.2 MPa, 60 °C	Impregnation	Shang et al. (2012)
Pd/glass beads	0.3 MPa, 50 °C	Ion exchange	Shen et al. (2011)
Pd/Al$_2$O$_3$	0.1 MPa, 55 °C	Impregnation	Kosydar et al. (2011)
Pd/ZrO$_2$-γ-Al$_2$O$_3$	0.2 MPa, 45 °C	Impregnation	Feng et al. (2008)
Ni-B/γ-Al$_2$O$_3$	0.3 MPa, 60 °C	Impregnation	Hou et al. (2004)
Pd/Al$_2$O$_3$, Pd/SiO$_2$-γ-Al$_2$O$_3$	0.1 MPa, 50 °C	Impregnation	Feng et al. (2010)
Pd/ZAL	0.3 MPa, 75 °C	Co-precipitation, impregnation	Ingle et al. (2020b, 2021)
Pd/HCM	0.3 MPa, 75 °C	Co-precipitation, impregnation	Ingle et al. (2020a)

Fig. 3 Reaction scheme for cyclic reduction and oxidation of EAQ and THEAQ
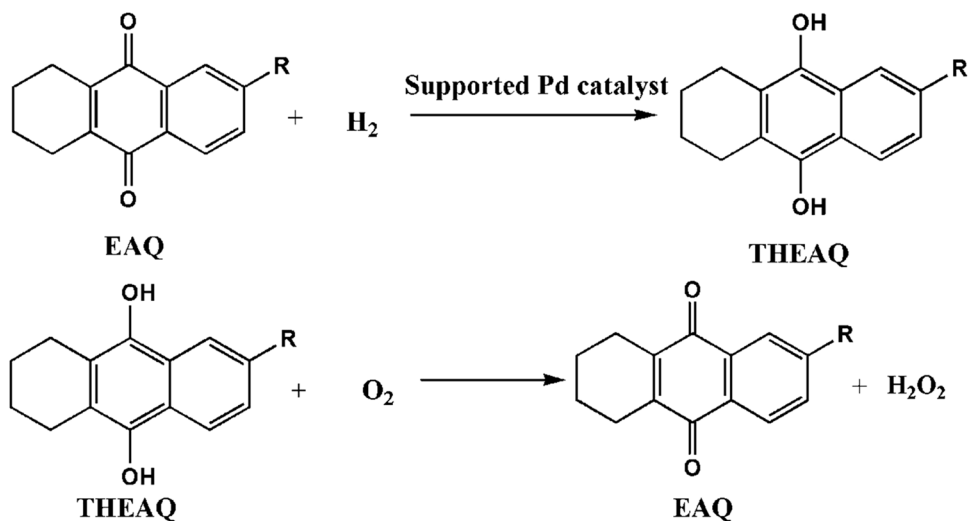
with aromatic rings partially hydrogenated and precipitated with EAQ molecules on the catalyst surface. The ring hydrogenation reactions are given in Fig. 4. 2-Ethyloctahydro-9,10-anthrahydroquinone (H_8EAQH_2) cannot be converted into H_2O_2. Hence, the other intermediate reactions have to occur to give anthrones and dianthrones (Ulmann 1994). A modified reaction is given in Fig. 5. Santacesaria et al. (1994b) mentioned that the EAQ inhibited the formation of H_8EAQH_2. The ring hydrogenation reaction of the aromatic rings of EAQ molecules in the presence of the Pd catalyst follows a dual-site mechanism at lower temperature and pressure as shown in Fig. 6 (Santacesaria et al. 1999, 1995).

Chen et al. (2015) prepared the Pd/γ-Al$_2$O$_3$ catalysts by the adsorption-reduction method and used in the hydrogenation of EAQ. CP extract which was used for the adsorption-reduction method can also be treated as a reductive and protective agent in the hydrogenation of EAQ. They performed the several experiments to find the effect of various parameters like reaction temperature, pressure, hydrogenation time, Pd loading, the volume of working solution, the flow rate of H_2, and the support modified by pretreatment on the yield of H_2O_2 and active EAQ contents. It was found that the highest yield of H_2O_2 could be achieved at optimized values of the working solution of 10 mL, the hydrogenation time of 1.5 h, and the flow rate of H_2 of 40 mL min^{-1} operated at 40 °C. The sufficient work had been carried out on the pretreatment with different alkali modifiers (Na$_2$SiO$_3$) on the γ-Al$_2$O$_3$-supported catalysts which show better catalytic activity (Drelinkiewicz et al. 2004a, 2004b). It was found that the different pretreated catalyst supports (HCl, NaOH, Na$_2$CO$_3$, and Na$_2$SiO$_3$) provide the different values of H_2O_2 yield with the enhancement of about 5–10%. However, Na$_2$SiO$_3$-pretreated supports provide the highest value of yield of H_2O_2 (96.4%). The pretreated catalyst supports can also reduce the formation of the degradation products.
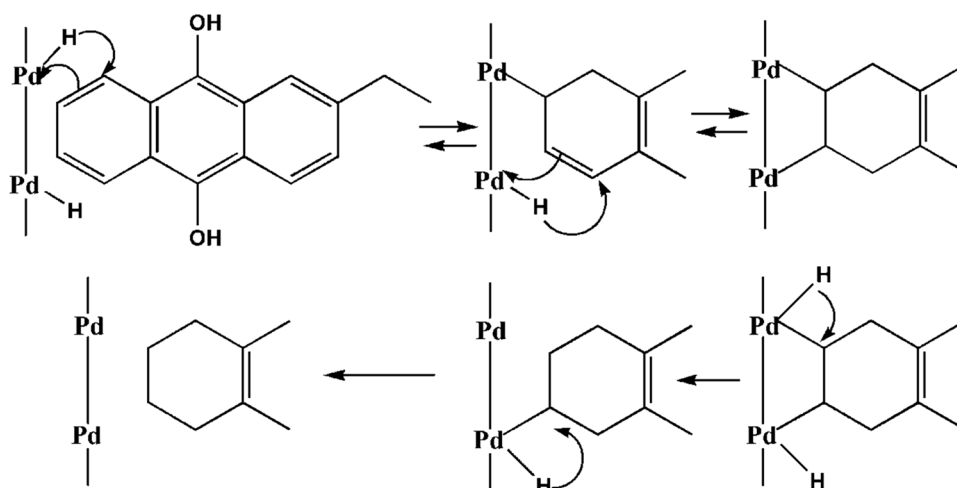

Fig. 4 Reaction scheme for ring hydrogenation
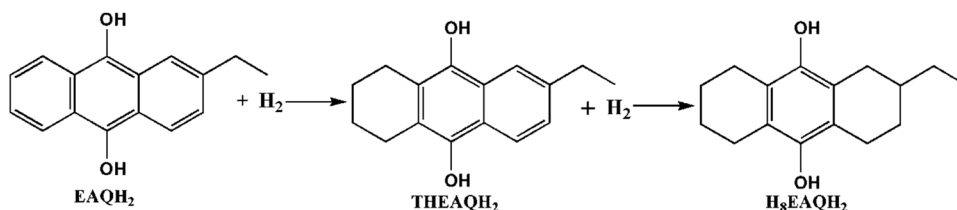
Fig. 5 A simplified reaction scheme for hydrogenation of EAQH$_2$
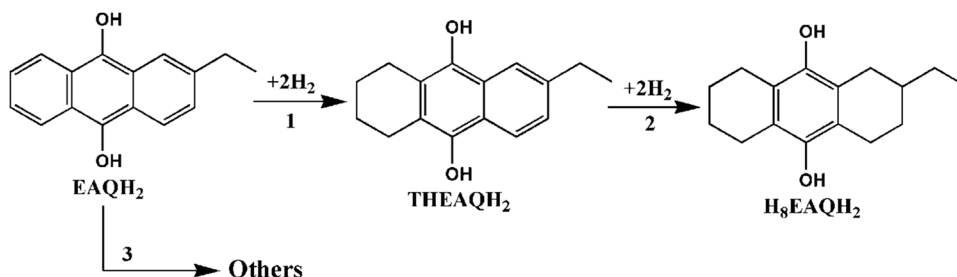
Fig. 6 Schematic representation of the dual-site mechanism

2-Amyl anthraquinone (AAQ) was hydrogenated in the presence of the Pd catalyst prepared by the polyol synthesis method. The effect of the size of the catalysts has also been studied in terms of the selectivity of the catalyst. The production of H_2O_2 by the AQ process needs to be focused on the selectivity of the catalyst. The consumption of active quinone in the hydrogenation/oxidation process increases with the generation of degradation products, leading to the decrease in catalyst activity. The bigger size particles easily activate the C=O bond, though AAQ has a unique configuration with reaction centers to activate the carbonyl group or aromatic ring. Also, the larger size of the Pd catalyst promotes the rate of deactivation which may be attributed to numerous side reactions (Li et al., 2016a, b).

Similarly, Yuan et al. (2016) have used one-pot evaporation-induced self-assembly (EISA), and hydrothermal (HT) methods for the synthesis of a Pd/Al_2O_3 catalyst by using the typical synthesis process of impregnation. The one-pot synthesis method provides the higher specific surface area, precise mesopores with the confined distribution of the pores, and the Pd particles effectively encapsulated over the inner part of the mesopores of Al_2O_3. Most probably, Pd and Pd black catalysts with and without supports have been used after the Rn-Ni catalyst by most of the manufacturers (Edvinsson Albers et al., 2001). The size and dispersion of the Pd particles are the essential variables to decide the activity of the supported catalysts. The dispersion of the Pd particles depends upon some of the favorable conditions such as the higher surface area of the support, uniform pore structure, and smaller pore size distribution. The elemental characteristics of the supports affect the dispersion of the Pd particles, which depends on the catalyst precursors (Tang et al. 2014), preparation methods (Li et al. 2012, 2014; Hong et al. 2015), and chemical compositions (Feng et al. 2010) of the catalysts.

Drelinkiewicz and Waksmundzka-Gora (2006a, b) performed the hydrogenation of EAQ with various catalyst supports such as Pd/C, Pd/SiO_2, and Pd/Al_2O_3. It was found that the catalyst with alumina support provides the higher catalyst activity. The selectivity towards active quinone and the generation of undesirable products get affected by the acidity of the support, whereas the acidity of the Al_2O_3-supported catalyst decreases the formation of undesirable products and enhances the selectivity of hydrogenation reaction (Yuan et al. 2016). The alumina-supported metal oxide composites have been prepared by HT or EISA synthesis processes for the numerous applications in the catalysis (Xu et al. 2012). Yuan et al. (2016) systematically studied the hydrogenation of EAQ using four types of catalysts. The higher catalyst activity was observed in the hydrogenation reaction in case of smaller Pd particles size (Feng et al. 2010). However, the surface morphologies and the electronic state of Pd particles affect the catalyst activity more than the size of particles.

Thus, the increase in the catalytic activity may be attributed to the greater electron density of Pd particles at the interface.
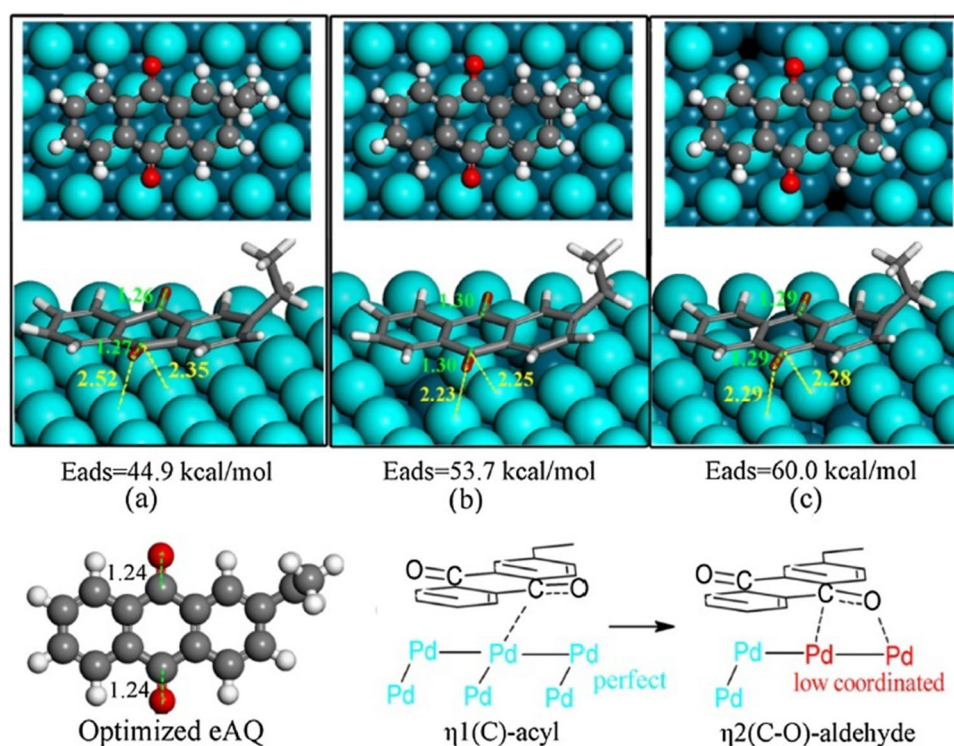
The adsorbed EAQ structure on perfect Pd and the low coordinated Pd were evaluated by density functional theory (DFT). Figure 7 describes the most stable structure of EAQ adsorption. It has two benzene rings and carbonyl oxygen atoms of EAQ located at bridge sites, along with the elongation of the carbonyl bond (0.03 Å) on the perfect Pd(111) surface. The distance between the carbonyl oxygen atom and the nearest Pd atom ($Oc-Pd_{On}$) is longer than the distance between the carbonyl carbon atom and the nearest Pd atom ($Cc-Pd_{Cn}$). Hence, it can be confirmed the formation of an acyl intermediate (η^1(C)-acyl) on the Pd(100) surface. The EAQ adsorption energy was found to be increased over low-coordinate Pd atoms (53.7 kcal/mol and 60.0 kcal/mol). The elongation of the carbonyl bond from 0.05 to 0.06 Å might be the reason to decrease the distance between Oc-PdOn and Cc-PdCn. Also, Fig. 7c confirms the formation of a di-sigma complex (η^2(C–O)-aldehyde), when the distance between $Oc-Pd_{On}$ and $Cc-Pd_{Cn}$ almost vanishes. Hence, the hydrogenation of EAQ using low-coordinated Pd atoms allows the possible adsorption of the EAQ structure.

In the past, many researchers focused on the improvement of the catalytic activity due to the synergetic effect (Alonso et al. 2012) of the incorporation of second metal to the Pd-based catalyst (Au (Yang et al. 2012; Kittisakmontree et al. 2013), Ag (Zhang et al. 2000), and Pt (Kim et al. 2014; Xu et al. 2012)). Zhang et al. (2017) observed the promotion of hydrogenation reaction due to the introduction of the second metal with the Pd catalyst. The addition of Ru on Pd improved the hydrogenation efficiency of the Pd catalyst with higher selectivity toward active quinone. It also increases the desorption of hydrogen atoms as compared to single-Pd-based catalysts. They confirmed that the promotion effect of bimetallic Pd-Ru catalysts improves the catalytic activity of Pd-based catalysts. It was found that both the catalyst activity and selectivity have been improving with the incorporation of Ru to the Pd catalyst in the hydrogenation of EAQ.

The superior performance of Pd-Ru catalysts can be attributed to the adsorption of H_2 and the activation of C=O bond in the hydrogenation of EAQ. The dissociative adsorption of the H_2 molecules provides the hydride ions to the surface of the Pd and Ru catalyst which enhances the reaction activity. The proposed mechanism for adsorption of H_2 and activation of the C=O bond of the aromatic ring of EAQ on the surface of the catalyst may be due to the lone pair of electrons of the oxygen atoms of Pd^{2+} and Ru^{4+} acting as an electrophilic site and hence improves the performance of Pd-Ru catalysts (Fig. 8).

Han et al. (2015a) prepared single-crystal Pd nanocrystals over the immobilized γ-Al_2O_3 catalyst with exposed (100) and (111) facets which were used in the hydrogenation of

Fig. 7 DFT-optimized structures of EAQ (down left), adsorbed EAQ on perfect (**a**) and defective (**b**) and **c** Pd(111) facets. Red, gray, white, and blue spheres represent O, C, H, and Pd atoms, respectively (light blue stands for the top layer) (Yang et al. 2012) (reprinted with permission)

Eads=44.9 kcal/mol (a)   Eads=53.7 kcal/mol (b)   Eads=60.0 kcal/mol (c)

Optimized eAQ   η1(C)-acyl   η2(C-O)-aldehyde

Fig. 8 The proposed mechanism of promoting effect of a second metal in bimetallic Pd-Ru/γ-Al$_2$O$_3$ samples and the preferential modes of 2-ethylanthraquinone activation on their surface (Jin et al. 2012). Reprinted with permission
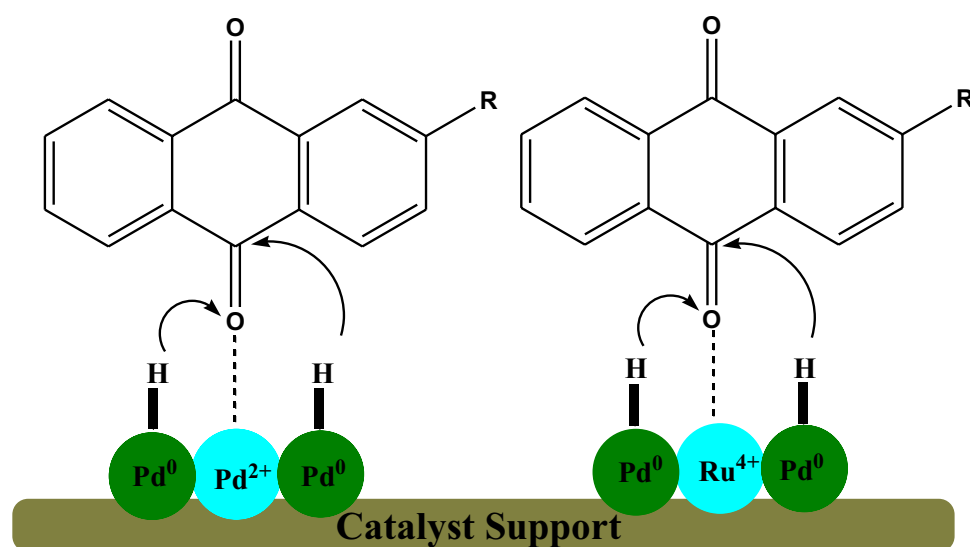

EAQ. Both Pd(100) and Pd(111) facets were simultaneously more active toward the hydrogenation of C=O and the activation of the aromatic ring in EAQ. Hence, single-Pd nanocrystals were prepared by one-step synthesis and used in the hydrogenation of EAQ (Tan et al. 2012). It can handle the Pd(100) facet exposure and enhance the stability of Pd metal components. The principal mechanism of hydrogenation reaction of EAQ involved two important steps: the activation of the C=O bond of the aromatic ring of EAQ and adsorption of H$_2$ molecules. The previous studies reveal that the low-coordinate Pd(111) facet is less active in the adsorption and activation of H$_2$ molecules than the perfect Pd(100) facet. However, there are no studies related to the activation of EAQ by Pd catalysts. Figure 9 describes the modified adsorbed structures of EAQ over the Pd(100) and the Pd(111) facets. The stability of the Pd catalyst was found to be improved due to an increase in the interactions between the support and the nanocrystals formed by using the one-step synthesis method.

The incorporation of Au into the Pd/Al$_2$O$_3$ catalyst with the combination of IM and DP methods can enhance the catalytic activity and selectivity for the hydrogenation of

Fig. 9 Optimized structures of EAQ adsorbed on the **a** Pd (100) and **b** Pd (111) surfaces (Tan et al. 2012). Reprinted with permission
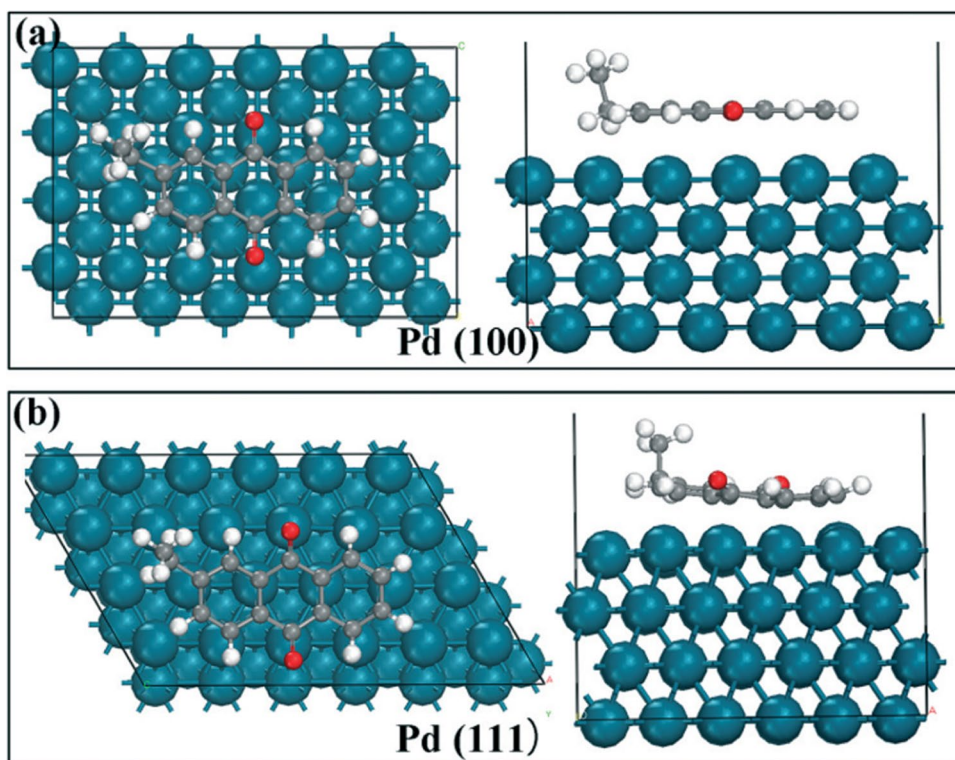
EAQ (Han et al. 2015a). Au remained inactive for the EAQ hydrogenation which was confirmed by the negligible yield of 1.11 g L^{-1} for the Au/Al$_2$O$_3$ catalyst. It indicates that the Au atom was neutral, but after loading with the Pd atom, it could provide a significant amount of charge transfer to the Al$_2$O$_3$ surface, leading to enhancement of the oxidation of Pd. When Au was being added to the Pd/Al$_2$O$_3$ catalyst, the Pd/Au/Al$_2$O$_3$ (14.27 g L^{-1}) and Au/Pd/Al$_2$O$_3$ (12.79 g L^{-1}) catalysts have exhibited higher hydrogenation efficiency than Pd/Al$_2$O$_3$ (12.04 g L^{-1}). Li et al. (2012) developed highly dissipated Pd/Al$_2$O$_3$ catalysts with large surface area and the flowerlike shape design whisker alumina supports. The alumina crystallites can be activated on top of the alumina surface after the evolution of OH$^-$ ions by decomposition of urea. Then, activated Al^{3+} mixed with an aqueous solution of NH$_3$ and CO$_2$ to form ammonium aluminum carbonate hydroxide NH$_4$[Al(OOH)HCO$_3$] nanocrystals. The higher hydrogenation efficiency and selectivity of EAQ hydrogenation is reported with whisker-modified alumina. The formation of degradation products affects the hydrogenation efficiency as the reaction time proceeds (Biasi et al. 2010).

Hong et al. (2015) have involved a low potential-anodizing method to prepare anodic alumina oxide (AAO) supports. They prepared θ-ring-shaped Pd/AAO@Al catalysts by impregnating the Pd catalyst over AAO supports. The controlled preparation method involved different anodizing potentials over a reaction time to adjust the pore size and depth of the prepared AAO supports. In this case, the diffusion is the main driving force for the reaction to occur. The external and internal mass transfers for the hydrogenation reaction of EAQ by using various heterogeneous catalysts, mainly supported Pd catalysts, usually depend upon the shape and pore structure of the support. The performance of the Pd/AAO@Al catalysts in the hydrogenation of EAQ has been enhanced due to the confined effect of cylindrical-shaped pores arranged in a highly ordered array in the AAO support with narrower diffusion distance.

The hydrogenation of AQ and THAQ can be estimated using DFT calculations. The cluster models (Christmann, 1988; Baykara et al. 1986; Rochefort et al. 1990; Roques et al. 2001, 2007; Bertin et al. 2005) and slab models (Dong et al. 1996; Kamachi et al. 2013) were used to investigate the behavior of the Pd(111) facet (Kamachi et al. 2015). The Pd atoms can adsorb atomic H$_2$ to form H$_2$ atoms with the two neighboring 3-fold hollow fcc positions. The H$_2$ dissociation is facile, and the adsorbed AQ remains at the bridge sites on the Pd(111) surface (Kamachi et al. 2015). Thus, anthrahydroquinone (AHQ) and tetrahydroanthrahydroquinone (THAHQ) could be formed with the combination of the two carbonyl O$_2$ atoms of AQ and THAQ with the surface H$_2$ atoms. The Pd catalyst with various supports (C, SiO$_2$, and Al$_2$O$_3$) has been used in the hydrogenation of AQ and THAQ to form AHQ and THAHQ (Santacesaria et al. 1994a, 1994b; Albers et al. 2001; Fajt et al., 2008). The hydrogenation of THAQ is reported as more productive than that of AQ to convert into THAHQ and the degradation of

AQ and THAQ to form degradation products such as tetrahydroanthrone (THAN), anthrone (AN), tetrahydro-oxanthrone (THOAN), and oxanthrone (OAN) which were slow (Santacesaria et al. 1988). Hence, demand is growing for process intensification for an industrial AQ process where the side reactions could be suppressed.

SiO$_2$-supported catalysts

Silica supports have been used in the field of catalysis due to its excellent properties. Highly dispersed catalysts can be prepared using silica as supporting material. It has enormous properties like high surface area and high pore volume, and the mesoporous channels make them comfortably used for impregnation of metal catalyst for better adsorption and dispersion of metal salt and trap active metal particles that can resist deactivation during the reaction.

Hydrogenation of EAQ by using the Pd/SiO$_2$ catalyst has been carried out with almost 100% selectivity in a slurry reactor. Drelinkiewicz (1992) investigated the effect of catalyst dosages on the rate of hydrogenation, the yield of 2-ethyltetrahydro-9,10-anthrahydroquinone (H$_4$EAQH$_2$), and the formation of the degradation products. It indicates that the formation of EAQH$_2$ is dependent on the intermediate product H$_4$EAQH$_2$. It was found that the average value of degree of hydrogenation for the generation of degradation products can be evaluated from the individual degree of hydrogenation (U). The value of U changes during reaction, depending on the amount of catalyst. Hence, the formation of degradation products or undesirable products due to side reaction depends on the catalyst concentration.

The selectivity towards active quinone in the hydrogenation of EAQ can be determined by the concentration of H$_2$ on the surface of the catalyst and the type of reaction regime used. Mainly, two types of reaction regimes can be used in the hydrogenation reaction such as kinetically controlled and diffusion-controlled regimes. The "hydrogen poor" mode has observed when the rate of reaction was associated with the rate of H$_2$ transport. However, the "hydrogen-rich" mode existed when the rate of the chemical reaction was interpreted by the overall reaction rate. Ni catalyst has been dealt with the hydrogenation of AQ under high pressure of H$_2$ with the quantitative formation of AN. Hydrogenation of AQ on Pd/Al$_2$O$_3$ and Pd/SiO$_2$-Al$_2$O$_3$ could also form H$_4$EAQ and other unidentified products. Drelinkiewicz (1992, 1995) investigated in the deep hydrogenation of AQ that the temperature, the catalyst dose, and the grain size can manage the internal diffusion, or external mass transport processes and the chemical reaction. The different reaction regimes can have different impacts on the hydrogenation reaction and, more specifically, the yield of H$_4$EAQ. The yield of H$_4$EAQ increases when the external mass transport is the driving force for the reaction kinetics involved (Binder et al. 2009).

Drelinkiewicz et al. (2004a, b, 2005, 2007) studied extensively the SiO$_2$ and Al$_2$O$_3$-supported eggshell catalysts with various types of supports and Pd concentration profile in the hydrogenation of EAQ. The precipitation technique was used to precipitate palladium hydroxide onto SiO$_2$ and Al$_2$O$_3$ supports to prepared catalysts which were then impregnated with various alkaline (NaHCO$_3$, NaH$_2$PO$_4$, Na$_2$SiO$_3$) solutions. The SiO$_2$-supported catalyst provides poor deactivation than the Al$_2$O$_3$-supported catalysts, whereas the SiO$_2$-Al$_2$O$_3$-mixed supported catalyst with Na$_2$SiO$_3$ impregnation gives the better catalyst activity (Drelinkiewicz et al. 2004a, 2004b, 2006a,b).

The hydrogenation of EAQ has also been found to be affected consequently by the humidity. The humidity plays a crucial role in the hydrogenation reaction, the dissociation of EAQ to EAQH$_2$, and also the conversion of EAQH$_2$. The utilization of EAQH$_2$ and desirable and undesirable products varies depending upon the alkalinity of Pd/SiO$_2$ catalysts. The humidity dominates the process of EAQH$_2$ transformation with less-alkalinity Pd catalysts.

Advanced catalytic systems

The mass transfer of EAQ in the hydrogenation of EAQ using the Pd catalyst is a fast reaction and rate-controlling step (Santacesaria et al. 1988). On this prediction, Feng and co-investigator (2010) performed the hydrogenation of EAQ in a slurry reactor using the newly synthesized catalyst Pd/SiO$_2$-Al$_2$O$_3$, which can attain 10.3 g L^{-1} of the yield of H$_2$O$_2$. Shen et al. (2011) achieved 11.2 g L^{-1} of the yield of H$_2$O$_2$ with a Pd/eggshell glass catalyst. The particle size can be controlled by varying the reflux timing and the calcination temperature (Yuan et al. 2016). As catalytic properties of catalyst depend upon the surface structure and particle size, the focus on the design of catalysts is desirable for well-defined highly dispersed particles. The correlation between the particle size and the reaction activity or selectivity has been introduced by various authors (Binder et al. 2009; Zhou et al. 2006).

Eggshell structure catalysts used in the hydrogenation of EAQ decrease the diffusion distance to enhance the reaction rate. Carbon or Al$_2$O$_3$ supports have been used for the commercial Pd catalysts in the conventional processes. The acidity of the support material has imparted a specific role in the hydrogenation reaction. Shen et al. (2011) have used eggshell-structured glass beads to support the Pd catalyst. They have used subcritical water treatment as the pretreatment of support and the ion exchange method for loading Pd metal. The hydrogenation reaction was performed in a fixed-bed reactor packed with a Pd-supported eggshell catalyst. The metal ions contained in glass beads exchange with the metal ions with higher electronegativity. Sixty percent of conversion of EAQ was achieved in less than 2 s at a liquid

flow rate of 0.6 mL min^{-1}, gas-to-liquid ratio of 30, and Pd loading of 0.34 wt%. The space-time yield (STY) and hydrogenation efficiency were found to be 3800 $g_{H_2O_2}$ g_{Pd}^{-1} h^{-1} and 11.2 $g_{H_2O_2}$ L^{-1}, respectively. A similar study has been done by Yao et al. (2016a) for the hydrogenation of EAQ by using the eggshell structure of the Pd catalyst in a fixed-bed reactor. In situ prepared catalyst has a diameter of 100 μm, shell thickness of 3–4 μm, and small mono-dispersed Pd nanoparticles ranging from 4 to 5 nm. The hydrogenation efficiency of 6.6 g L^{-1} and the yield of H$_2$O$_2$ of 35.5% were obtained at an optimum Pd content of 0.32% and a residence time of less than 4 s. Thiele modulus and effective internal diffusion factors were used to know the effect of internal diffusion resistance. It was found that it weakens the internal diffusion resistance for fast reactions. The STY for hydrogenation reaction was found to be 567.5 $g_{H_2O_2}$ g_{Pd}^{-1} h^{-1} at the liquid flow rate of 0.2 mL min^{-1} and the gas-to-liquid ratio of 30.

The monolithic catalysts have been used extensively in various catalytic reactions. The basic characteristic of the ideal monolithic catalyst consists of enough durability, high specific surface area, and catalytically active phases. The structure of the porous layer plays an important part in the enlargement of the surface area of the catalyst and affects the active phase required for catalysis. The catalytically active phase in the monolithic catalyst improves the active sites needed for chemical reactions due to its high distribution capacity. Zhang et al. (2008) compared a novel Pd/Al$_2$O$_3$/cordierite monolithic catalyst with the Pd catalyst having Al$_2$O$_3$ coating. It was found that the STY of H$_2$O$_2$ over a monolithic catalyst is better than that of commercial catalysts with only Al$_2$O$_3$ coating. In the hydrogenation of EAQ using the monolithic catalyst, the diffusion distance is very short which improves the diffusion of the active metal. Li et al. (2015) have performed the 1000-h-long stability runs and determined that the monolithic catalyst with SiO$_2$ coating (PSC) provides better catalytic activity than the Al$_2$O$_3$ coating (PAC). The regular structure and weak acidity of the PSC monolithic catalyst made them durable in such a long test. The yield of H$_2$O$_2$ increases up to 5.5 g L^{-1} with the incorporation of MgO to the SiO$_2$ wash coat (Li et al. 2016a, b). It was also investigated that the mass transfer distance was very short and the mass transfer resistance also becomes less in the case of monolithic catalyst, leading to the improved hydrogenation efficiency. Thus, the application of a monolithic catalyst in the hydrogenation of EAQ has an important contribution.

Shi et al. (2016) investigated the Pd/oxide/cordierite monolithic catalysts prepared by the impregnation method. The Al$_2$O$_3$ layer with about 6 μm of the modest thickness in the prepared catalyst was used in the flowing tube reactor for hydrogenation of EAQ. The highest conversion of EAQ was found to be 99.1%, and the hydrogenation efficiency was found to be 10.0 g L^{-1}. It resulted to the successful Pd penetration and the wider pore size, which promotes the distribution of Pd and receptiveness of the active sites by the reactants. The catalyst activity generally depends upon the type and thickness of the oxide layer. The catalyst with γ-Al$_2$O$_3$ as a layer gives higher reactivity than SiO$_2$ and SiO$_2$-Al$_2$O$_3$ as layers.

The metal-organic frameworks (MOFs) and modified zeolites have been introduced for the hydrogenation of EAQ. The ordered structure, higher surface area, and constant distribution of pore size of the zeolites (e.g., MCM-41 and SBA-15) make them better to support Pd nanoparticles and reduce the diffusion resistance. It enhances the surface for systematic dispersion of metal in the three-phase catalytic reactor (Beck et al. 1992; Kresge et al. 1992; Tanev and Pinnavaia, 1996). Guo et al. (2017) determined the pore diameter of zeolites (MCM-22 and Beta) and the effect on the EAQ hydrogenation. It was found that the monolithic catalyst (0.8% Pd/MCM-41/COR) demonstrated the highest yield of H$_2$O$_2$ (7.54 g L^{-1}) and selectivity (85.3%) in the production of H$_2$O$_2$ by AQ process. The efficiency of 0.8% Pd/MCM-41/COR monolithic catalyst (1573 $g_{H_2O_2}$ g_{Pd}^{-1} h^{-1}) was much higher than that of a commercial pellet catalyst (500 $g_{H_2O_2}$ g_{Pd}^{-1} h^{-1}). The monolithic catalysts possess higher mass transfer coefficients (5–20 times) than the commercial catalyst. Guo et al. (2016) have presented the hydrogenation of EAQ using monolith catalysts (Pd/SiO$_2$/COR) with low-pressure drop which has a great impact on the mass transfer performance than the commercial pellet catalyst. It was found that the maximum STY obtained was 793.2 $g_{H_2O_2}$ g_{Pd}^{-1} h^{-1} with 1.5% Pd/SiO$_2$/COR catalyst at 80 °C and atmospheric pressure.

Cai et al. (2019) prepared the nanorod by adding EAQ to aluminum isopropoxide (AIP) and isopropyl alcohol (IPA). The characteristics of the support, structure of the catalyst, metal distribution, and the interactivity of the metal and the support are necessary factors to enhance the catalytic activity of hydrogenation reaction (Augustyn et al. 2010). The modification of the support is generally used to enhance catalytic activity. The results reveal that the addition of a certain fixed amount of EAQ (4 wt%) in the hydrogenation step helps in the modification of the textural properties of the supports. The hydrogenation efficiency is reported to improve from 7.49 to 10.28 g L^{-1}, which is 37.3% higher than the catalyst prepared without incorporation of EAQ. The formation mechanism of the Pd/γ-Al$_2$O$_3$ catalyst is shown in Fig. 10. In this, EAQ was added to AIP and IPA and followed by the vigorous blending. Hydrolysis of AIP converts it into γ-AlOOH during the sol-gel process. In the aging process, the EAQ molecules were adsorbed on the crystals formed. The recognition effects of the addition of the structure-directing agent (EAQ) before the formation of
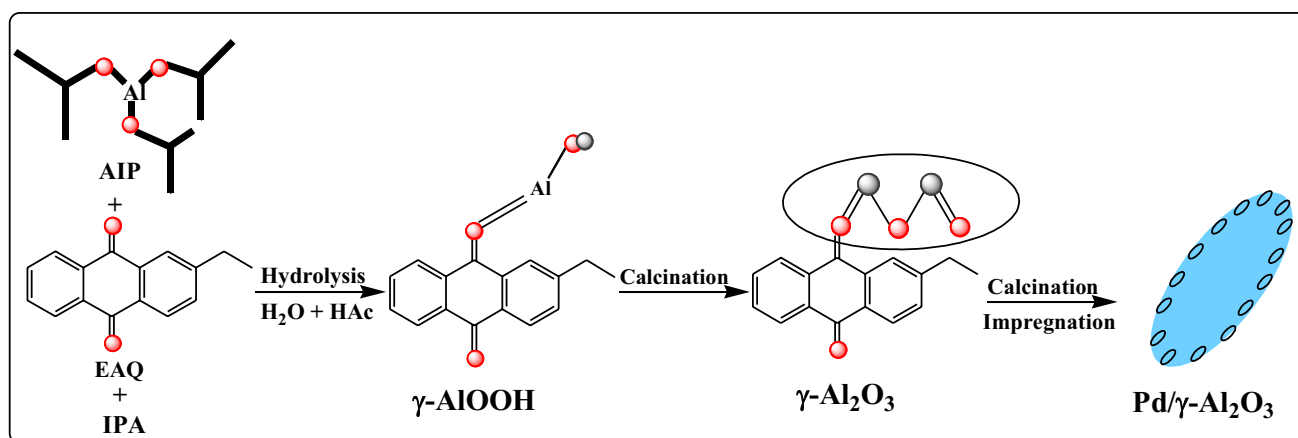
Fig. 10 Schematic representation of the EAQ-directed development mechanism of the Pd/γ-Al$_2$O$_3$ catalyst (Li et al. 2018). Reprinted with permission

Al(OH)$_3$ and separation after calcination (550°C) towards γ-AlOOH (Li et al. 2013) generate a definite pore structure over the commercially used γ-Al$_2$O$_3$ supports.

Nano-hybrid catalysts (bimetallic and trimetallic) have been used for various hydrogenation reactions (Chen et al. 2015; Hong et al. 2017; Carvalho et al. 2004; Surisetty et al. 2010; Hungria et al., 2006; Toshima et al. 2007; Adams et al. 2007; Liew et al. 2019). The novel nano-hybrid trimetallic catalyst support Zr-Al-La (ZAL) was synthesized by co-precipitation and impregnated with Pd by an incipient wetness impregnation method (Ingle et al., 2020a, b, 2022). The hydrogenation reaction was performed in a high-pressure autoclave reactor with Pd supported on ZAL catalyst. The co-precipitation by the direct contact of oxide supports gained much attention due to its accessibility and economy. By this method of the preparation of trimetallic oxide support which precipitates with small size, narrow size distribution and high crystalline structure may be obtained. Pd/ZAL catalyst improves the catalytic activity (9.15 g L^{-1}) and provides the high selectivity (100%) simultaneously, which has ascendancy over existing processes. The hydrogenation of 2-EAQ provides the conversion as high as 93% with only 0.5 g of the catalyst with a hydrogenation efficiency of 9.15 g L^{-1} at operating conditions of 75 °C and 0.3 MPa.

The size of Pd particles plays a vital role in controlling the activity of the catalyst, and the smaller dimensions of Pd particles benefit the hydrogenation of EAQ (Feng et al. 2010). The Pd supported on hollow ceramic microsphere (HCM) exhibits high catalytic activity, selectivity, and stability in the liquid-phase hydrogenation of EAQ (Ingle et al. 2020, 2021). Catalytic activity was found to be 9.42 g L^{-1} with 100% selectivity over the Pd/HCM catalyst. The calculated mass transfer resistance of the reaction over the Pd/Zr-Al-La catalyst was found to be moderate with a diffusion coefficient of the reactant (H$_2$) of 0.0133×10^{-6} m^2 s^{-1} at

75 °C. It was also verified and confirmed with the Thiele modulus (calculated as 0.0289) indicating no mass transfer resistance. The effectiveness factor (η_s) was found to be 1.0, indicating the negligible mass transfer resistance in the hydrogenation reaction using the Pd/HCM catalyst

Ma et al. (2019) grafted silica support (SBA-15) with alkyltriethoxysilane to support commercial Pd catalysts. The silica supports can be functionalized by grafting method with alkyltriethoxysilane and deposition of Pd by the incipient wetness impregnation method. Both the grafting sequence and the grafting amount were varied over each hydrogenation cycle. It was reportedly found that the grafting agent improves the catalytic activity by increasing the hydrophobicity of the silica support. The effect of grafting amount in the hydrogenation of EAQ over Pd/SBA-15 catalysts provides better performance. The highest grafting amount of catalysts gives the enhancement in the activity and the selectivity of the hydrogenation reaction (98.3%).

Conclusions

The hydrogenation of EAQ into EAQH$_2$ for the production of H$_2$O$_2$ gains more interest to meet the environmental demands of H$_2$O$_2$ as a green oxidant. The commercial production of H$_2$O$_2$ by the AO process proposed in Germany in the late 1930s has been used for large-scale production. The homogeneous catalysts (Ni, Cu, and Pd) have been used by many researchers in the hydrogenation of EAQ for the commercial production of H$_2$O$_2$ from the AO process, and it provided the satisfactory activity and selectivity. Moreover, the separation and regeneration of the catalysts were still complicated. Intensification and investigation of reaction mechanisms of the AO process are the utmost important issues for the technical development of liquid-phase

hydrogenation of EAQ in the presence of the Pd catalysts. Thus, the development of heterogeneous catalyst is relatively secondarily recognized in the field of catalysis. The development of the heterogeneous catalysts in the hydrogenation reactions is looked forward to increase the production of H_2O_2, as the heterogeneous catalysts were not used for commercial production of H_2O_2. Nonetheless, the H_2O_2 process needs to fortify further in wholesomeness. Therefore, the heterogeneous catalysts are designed to have better stability, easy separation, safe handling, regeneration of the catalyst, and the reactor designing, which optimized the costs of commercial production of H_2O_2.

The alumina-supported catalysts can be significantly applied for the production of H_2O_2 by the AQ process and in the direct synthesis of H_2O_2. The Al_2O_3-supported catalyst provides an enhancement in the efficiency of H_2O_2 synthesis in the AQ process. Al_2O_3-supported catalysts are reported to provide more yield of H_2O_2 than the conventional Ni- and Pd-based catalysts. These catalysts can show high activity than the conventional Pd catalysts. Bimetallic catalysts (Pd-Co, Pd-Ag, Pd-Cu, Pd-Au, Pd-Ru, Pd-La), amorphous alloys, and facet-controlled Pd nanocrystal catalysts gave better hydrogenation efficiency than the commercial pellet catalysts. The novel metal catalysts generally provide much higher activity in contrast with the oxide-supported catalyst at lower reaction temperatures. Furthermore, Pd-based catalysts with stronger interactions between promoter and the major component, definite structure, better metal dispersion, and superfine particle exhibits higher selectivity, stability, and catalyst activity in the hydrogenation of EAQ. Disregarding with process development in the structure of the catalyst, one must be focused on developing reactors designed to intensify the activity and selectivity of EAQ hydrogenation. In recent years, the fluidized-bed reactor has become the substitute for a fixed-bed reactor. The fluidized-bed reactor has been a trending technology with important findings used in the hydrogenation reaction of EAQ for the production of H_2O_2. Sinopec has developed hydrogenation reaction by using bimetallic supported catalysts in the fluidized-bed and slurry stirring tank reactor for the production of H_2O_2 (Li et al. 2018).

Cordierite monolith catalysts exhibit much higher selectivity towards active quinones (> 99%) and can be obtained over Pd/γ-Al_2O_3/cordierite monolithic catalysts at the reaction temperature of 60 °C and atmospheric pressure, however at a lower yield of H_2O_2 (10 g L^{-1}). Furthermore, the nanocrystals of Pd metal with oxide support provide better catalytic activity. Thus, the high solidity of the abovementioned catalyst in the hydrogenation of EAQ forged them better than metal-based catalysts. The maximum H_2O_2 yield was reported up to 15 g L^{-1} and was achieved over the Pd/Au/Al_2O_3 catalyst with 99.56% selectivity towards active quinones. Commercially, H_2O_2 can be produced from sequential auto-oxidation of EAQ with Pd-based catalysts, the technique which is often employed for useful production of H_2O_2. Nonetheless, numerous significantly active metal catalysts were employed for EAQ hydrogenation. The eminently promising hydrogenation catalyst with almost 100% selectivity was Pd/SiO_2. However, a substantial amount of investigation in the field of hydrogenation catalysts for EAQ hydrogenation has been carried out with analysis and theoretical interpretation, and the mechanism behind hydrogenation reaction is still invariance. The advancement in recent findings should have assuredly accentuated basic acknowledgment regarding the characteristics of active sites and the active component mutual actions of a catalyst booster including support mechanisms of reaction, which play a significant part in the highly effective catalyst designed for the hydrogenation of EAQ.

Author contribution Anjali A. Ingle: contribution in the conceptualization, collection of the literature, data analysis, and writing of the manuscript. Shahid Z. Ansari: formation of the figures and tables and editing of the manuscript. Diwakar Z. Shende: review of and correction in the manuscript. Kailas L. Wasewar: review of and correction in the manuscript. Aniruddha B. Pandit: critical review of and correction in the manuscript. All authors read and approved the final manuscript.

Declarations

Ethics approval and consent to participate Not applicable

Consent for publication All authors give consent to publish the present work as per publisher policy.

Competing interests The authors declare no competing interests.

References

Adams RD, Boswell EM, Captain B et al (2007) Bimetallic Ru–Sn nanoparticle catalysts for the solvent-free selective hydrogenation of 1,5,9-cyclododecatriene to cyclododecene. Angew Chemie Int Ed 46:8182

Albers RE, Nystrom M, Siverstrom M et al (2001) Development of a monolith-based process for H_2O_2 production: from idea to large-scale implementation. Catal Today 69:247

Alonso DM, Wettstein SG, Dumesic JA (2012) Bimetallic catalysts for upgrading of biomass to fuels and chemicals. Chem Soc Rev 41:8075

Asghar A, Raman AAA, Wan Daud WMA (2015) Advanced oxidation processes for in-situ production of hydrogen peroxide/hydroxyl radical for textile wastewater treatment: a review. J Clean Prod 87:826

Augustyn WG, McCrindle RI, Coville NJ (2010) The selective hydrogenation of acetylene on palladium-carbon nanostructured catalysts. Appl Catal A: Gen 388:1

Baykara NA, Andzelm J, Salahub DR, Baykara SZ (1986) Hydrogen chemisorption on, and diffusion through, palladium clusters. Int J Quantum Chem 29:1025

Beck JS, Vartuli JC, Roth WJ et al (1992) A new family of mesoporous molecular sieves prepared with liquid crystal templates. J Am Chem Soc 114:10834

Berglin T, Schoon NH (1981) Kinetic and mass transfer aspects of the hydrogenation stage of the anthraquinone process for hydrogen peroxide production. Ind Eng Chem Process Des Dev 20:615

Bertin V, Curz A, DelAngel G et al (2005) The H and H_2 interaction with Pd_3Cu, Pd_4, and Cu_4 fee (111) clusters: a DFT comparative study. Int Quantum Chem 102:1092

Biasi P, Pinna F, Menegazzo F et al (2010) Hydrogen peroxide direct synthesis: selectivity enhancement in a trickle bed reactor. Ind Eng Chem Res 49:10627

Binder A, Seipenbusch M, Muhler M, Kasper G (2009) Kinetics and particle size effects in ethene hydrogenation over supported palladium catalysts at atmospheric pressure. J Catal 268:150

Bremner DH, Burgess AE, Feng-Bin L (2000) Coupling of chemical, electrochemical and ultrasonic energies for controlled generation of hydroxyl radicals: direct synthesis of phenol by benzene hydroxylation. Appl Catal A: Gen 203:111

Cai W, Zhuo J, Fang J, Yang Z (2019) 2-Ethyl-9,10-anthraquinone assisted sol-gel synthesis of $Pd/\gamma-Al_2O_3$ nanorod with enhanced catalytic performance in 2-ethyl-9,10-anthraquinone hydrogenation. Chin J Chem Eng 27:1863

Carvalho LS, Pieck CL, Rangel MC et al (2004) Trimetallic naphtha reforming catalysts. I. Properties of the metal function and influence of the order of addition of the metal precursors on Pt–Re–Sn/γ-Al_2O_3–Cl. Appl Catal: A Gen:269:91

Centi G, Perathoner S, Abate S (2009) Direct synthesis of hydrogen peroxide: recent advances in modern heterogeneous oxidation catalysis. Wiley-VCH Verlag GmbH & Co. KGaA: Weinheim, Germany, pp. 253–287

Chalmers L (1996) Domestic and industrial chemical specialties. Leonard Hill, London, pp 67–69

Chen A, Zhu Q, Zhao Y, Tastumi Y, Iyoda T (2013) Novel catalysts of Au/SiO_2 hybrid nanorod arrays for the direct formation of hydrogen peroxide. Particle & Particle Systems Characterization 30:489

Chen H, Huang D, Su X et al (2015) Fabrication of $Pd/\gamma-Al_2O_3$ catalysts for hydrogenation of 2-ethyl-9,10-anthraquinone assisted by plant-mediated strategy. Chem Eng J 262:356

Cheng Y, Wang L, Lu S et al (2008) Gas-liquid-liquid three-phase reactive extraction for the hydrogen peroxide preparation by anthraquinone process. Ind Eng Chem Res 47:7414

Chidambara Raj CB, Quen HL (2005) Advanced oxidation processes for wastewater treatment: optimization of UV/H_2O_2 process through a statistical technique. Chem Eng Sci 60:5305

Christmann K (1988) Interaction of hydrogen with solid surfaces. Surf Sci Rep 9:1

Ciriminna R, Albanese L, Meneguzzo F et al (2016) Hydrogen peroxide: a key chemical for today's sustainable development. Chem Sus Chem 9:3374

Cui Y, Huang J, Fu X, Wang X (2012) Metal-free photocatalytic degradation of 4-chlorophenol in water by mesoporous carbon nitride semiconductors. Catal Sci Technol 2:1396

Debellefontaine H, Chakchouk M, Foussard JN, Tissot D, Striolo P (1996) Treatment of organic aqueous wastes: wet air oxidation and wet peroxide oxidation. Environ Pollut 92:155

Deng X, Wang C, Shao M, Xu X, Huang J (2017) Low-temperature solution synthesis of CuO/Cu_2O nanostructures for enhanced photocatalytic activity with added H_2O_2: synergistic effect and mechanism insight. RSC Adv 7:4329

Domingues FS, Freitas TKFDS, de Almeida CA et al (2017) Hydrogen peroxide-assisted photocatalytic degradation of textile wastewater using titanium dioxide and zinc oxide. Environ Technol 40:1223

Dong W, Kresse G, Furthmuller J, Hafner J (1996) Chemisorption of H on Pd(111): an ab initio approach with ultrasoft pseudo-potentials. J Phys Rev B 54:2157

Drelinkiewicz A (1992) Deep hydrogenation of 2-ethylanthraquinone over Pd/SiO_2 catalyst in the liquid phase. J Mol Catal 75:321

Drelinkiewicz A (1995) Kinetic aspects in the selectivity of deep hydrogenation of 2-ethylanthraquinone over Pd/SiO_2. J Mol Catal. A: Chem 101:61

Drelinkiewicz A, Hasik M (2001) 2-Ethyl-9,10-anthraquinone hydrogenation over Pd/polymers: effect of polymers–Pd(II) chloro-complexes interactions. J Mol Catal A: Chem 177:149

Drelinkiewicz A, Kangas R, Laitinen R et al (2004a) Hydrogenation of 2-ethylanthraquinone on alumina-supported palladium catalysts: the effect of support modification with Na_2SiO_3. Appl Catal A: Gen 263:71

Drelinkiewicz A, Pukkinen A, Kangas R, Laitinen R (2004b) Hydrogenation of 2-ethylanthraquinone over Pd/SiO_2 and Pd/Al_2O_3 in the fixed-bed reactor. The effect of the type of support. React Kinet Catal Lett 94:157

Drelinkiewicz A, Waksmundzka-Gora A (2006a) Investigation of 2-ethylanthraquinone degradation on palladium catalysts. J Mol Catal A: Chem 246:167

Drelinkiewicz A, Waksmundzka-Gora A (2006b) Hydrogenation of 2-ethyl-9,10-anthraquinone on Pd/SiO_2 catalysts: the role of humidity in the transformation of hydroquinone form. J Mol Catal A: Chem 258:1

Drelinkiewicz A, Waksmundzka-Gora A, Makowski W, Stejskal J (2005) Pd/polyaniline(SiO_2) a novel catalyst for the hydrogenation of 2-ethylanthraquinone. Catal Commun 6:347

Drelinkiewicz A, Waksmundzka-Gora A, Sobczak JW, Stejskal J (2007) Hydrogenation of 2-ethyl-9,10-anthraquinone on Pd-polyaniline(SiO_2) composite catalyst: the effect of humidity. Appl Catal A: Gen 333:219

Edvinsson Albers R, Nystrom M, Siverstrom M et al (2001) Development of a monolith-based process for H_2O_2 production: from idea to large-scale implementation. Catal Today 69:247

Fajt V, Kurc L, Cerveny L (2008) The effect of solvents on the rate of catalytic hydrogenation of 6-ethyl-1,2,3,4-tetrahydro-anthracene-9,10-dione. Int J Chem Kinet 40:240

Feng JT, Wang HY, Evans DG et al (2010) Catalytic hydrogenation of ethylanthraquinone over highly dispersed eggshell Pd/SiO_2–Al_2O_3 spherical catalysts. Appl Catal A: Gen 382:240

Feng W, Xu X, Suna K (2008) Hydrogenation of 2-ethylanthraquinone over Pd/ZrO_2-gamma-Al_2O_3 catalyst. React Kinet Catal Lett 93:135

Foller PC, Bombard RT (1995) Processes for the production of mixtures of caustic soda and hydrogen-peroxide via the reduction of oxygen. J Appl Electrochemistry 25:613

Freakley SJ, He Q, Harrhy JH et al (2016) Palladium-tin catalysts for the direct synthesis of H_2O_2 with high selectivity. Science 351:965

Gabriele C, Roland D, Siglinda P, Martin R (2003) Tubular inorganic catalytic membrane reactors: advantages and performance in multiphase hydrogenation reactions. Catal Today 79:139

Garcia-Serna J, Moreno T, Biasi P et al (2014) Engineering in direct synthesis of hydrogen peroxide: targets, reactors, and guidelines for operational conditions. Green Chem 16:2320

Gema BB, Montiel-Argaiz M, Desmedt F et al (2016) Direct synthesis of hydrogen peroxide with no ionic halides in solution. RSC Adv 6:99291

Gomes HT, Miranda SM, Sampaio MJ, Silva AMT, Faria JL (2010) Activated carbons treated with sulphuric acid: catalysts for catalytic wet peroxide oxidation. Catal Today 151:153

Goor G, Kunkel W, Weiberg O (1989) Ullmann's encyclopedia of industrial chemistry, (Eds: B. Elvers, S. Hawkins, M. Ravenscroft, and G. Schulz), VCH, Weinheim, pp. 443-466.

Guo Y, Dai C, Lei Z (2017) Hydrogenation of 2-ethylanthraquinone with monolithic catalysts: an experimental and modeling study. Chem Eng Sci 172:370

Guo Y, Dai C, Lei Z et al (2016) Synthesis of hydrogen peroxide over Pd/SiO2/COR monolith catalysts by anthraquinone method. Catal Today 276:36

Guo YY, Dai CN, Lei ZG (2019) Hydrogenation of 2-ethylanthraquinone on Pd-La/SiO2/cordierite and Pd-Zn/SiO2/cordierite bimetallic monolithic catalysts. Chem Eng Process Process Intensif 136:211

Han Y, He Z, Guan Y et al (2015a) Catalytic performance of PdAu/Al2O3 catalyst with special structural and electronic properties in the 2-ethylanthraquinone hydrogenation reaction. Acta Phys Chim Sin 31:729

Han Y, He Z, Wang S et al (2015b) Performance of facet-controlled Pd nanocrystals in 2-ethylanthraquinone hydrogenation. Catal Sci Technol. 5:2630

Hermans LAM, Geus JW (1979) Interaction of nickel ions with silica supports during deposition-precipitation. Stud Surf Sci Catal 3:113

Hong R, Feng J, He Y, Li D (2015) Controllable preparation and catalytic performance of Pd/anodic alumina oxide@Al catalyst for hydrogenation of ethylanthraquinone. Chem Eng Sci 135:274

Hong R, He Y, Feng Y, Li D (2017) Fabrication of supported Pd-Ir/Al2O3 bimetallic catalysts for 2-ethylanthraquinone hydrogenation. AIChE J 63:3955–3965. https://doi.org/10.1002/aic.15748

Hou Y, Wang Y, He F et al (2004) Effects of lanthanum addition on Ni-B/γ-Al2O3 amorphous alloy catalysts used in anthraquinone hydrogenation. App Catal A: Gen 259:35

Hungria AB, Raja R, Adams RD et al (2006) Angew Chemie Int Ed 45:4782

Immanuel CD, Doyle FJ, Cordeiro CF, Sundaram SS (2003) Population balance PSD model for emulsion polymerization with steric stabilizers. AIChE J 49:1392

Ingle AA, Ansari SZ, Shende DZ et al (2020a) Hydrogenation of 2-ethylanthraquinone with Pd supported on hollow ceramic microsphere catalyst: an experimental and kinetic study. J Indian Chem Soc 97:1033

Ingle AA, Ansari SZ, Shende DZ et al (2020b) Palladium supported on nano-hybrid Zr–Al–La catalyst for hydrogenation of 2-ethylanthraquinone. Indian Chem Eng 64:387. https://doi.org/10.1080/00194506.2020.1749141

Ingle AA, Shende DZ, Wasewar KL (2021) Synthesis, characterization, and application of hollow ceramic microsphere based Pd catalyst for hydrogenation of 2-ethylanthraquinone. J Indian Chem Soc 98:100177. https://doi.org/10.1016/j.jics.2021.100177

Ingle AA, Shende DZ, Wasewar KL et al (2022) Performance of Pd catalyst supported on trimetallic nanohybrid Zr–Al–La in hydrogenation of ethylanthraquinone. Int J Chem React Eng. https://doi.org/10.1515/ijcre-2021-0271

Isaka Y, Yamada Y, Suenobu T et al (2016) Production of hydrogen peroxide by the combination of semiconductor-photocatalyzed oxidation of water and photocatalytic two-electron reduction of dioxygen. RSC Adv 6:42041

Jennings SR, Dollhopf DJ, Inskeep WP (2000) Acid production from sulfide minerals using hydrogen peroxide weathering. Appl Geochem 15:35

Jiajian P, Feng S, Yanlong G, Youquan D (2003) Highly selective and green aqueous–ionic liquid biphasic hydroxylation of benzene to phenol with hydrogen peroxide. Green Chem 5:224

Jin MS, Zhang H, Xie ZX, Xia YN (2012) Palladium nanocrystals enclosed by {100} and {111} facets in controlled proportions

and their catalytic activities for formic acid oxidation. Energy Environ Sci 5:6352

Jose MCM, Gema BB, Jose LGF (2006) Hydrogen peroxide synthesis: an outlook beyond the anthraquinone process. Angew Chem Int Ed 45:6962

Kamachi T, Ogata T, Mori E et al (2015) Computational exploration of the mechanism of the hydrogenation step of the anthraquinone process for hydrogen peroxide production. J Phys Chem C 119:8748

Kamachi T, Shimizu K, Yoshihiro D et al (2013) Oxidation of silanes to silanols on Pd nanoparticles: H2 desorption accelerated by a surface oxygen atom. J Phys Chem C 117:22967

Karmakar SR (1999) Chapter 6, Bleaching of textiles. In: Chemical technology in the pre-treatment processes of textiles. Elsevier: Amsterdam, The Netherlands. 12, pp. 160–216

Kim E, Jeong HS, Kim BM (2014) Efficient chemoselective reduction of nitro compounds and olefins using Pd–Pt bimetallic nanoparticles on functionalized multi-wall-carbon nanotubes. Catal Commun 45:25

Kirchner JR (1979) Kirk-Othmer encyclopedia of chemical technology. Vol. 13, 3rd Ed. Wiley, New York, pp. 12-38

Kittisakmontree P, Pongthawornsakun B, Yoshida H et al (2013) The liquid-phase hydrogenation of 1-heptyne over Pd–Au/TiO2 catalysts prepared by the combination of incipient wetness impregnation and deposition–precipitation. J Catal 297:155

Kosydar R, Drelinkiewicz A, Ganhy JP (2010) Degradation reactions in anthraquinone process of hydrogen peroxide synthesis. Catal Lett 139:105

Kosydar R, Drelinkiewicz A, Lalik E, Gurgul J (2011) The role of alkali modifiers (Li, Na, K, Cs) in activity of 2% Pd/Al2O3 catalysts for 2-ethyl-9,10-anthraquione hydrogenation. Appl Catal A: Gen 402:121

Kresge CT, Leonowicz ME, Roth WJ et al (1992) Ordered mesoporous molecular sieves synthesized by a liquid-crystal template mechanism. Nature 359:710

Kumar A, Kumar A, Sharma G et al (2017) Solar-driven photodegradation of 17-β-estradiol and ciprofloxacin from waste water and CO2 conversion using sustainable-char/polymeric-g-C3N4/rGO metal-free nano-hybrids. New J Chem 41:10208

Li H, Zheng B, Pan Z et al (2018) Advances in the slurry reactor technology of the anthraquinone process for H2O2 production. Front Chem Sci Eng 12:124

Li J, Yao H, Wang Y, Luo G (2014) One-step preparation of Pd-SiO2 composite microspheres by the sol–gel process in a microchannel. Ind Eng Chem Res 53:10660

Li X, Su H, Ren G, Wang S (2015) A highly stable Pd/SiO2/cordierite monolith catalyst for 2-ethyl-anthraquinone hydrogenation. RSC Adv 5:100968

Li X, Su H, Ren G, Wang S (2016a) Effect of metal dispersion on the hydrogenation of 2-amyl anthraquinone over Pd/Al2O3 catalyst. J Braz Chem Soc 27:1060

Li X, Su H, Ren G, Wang S (2016b) The role of MgO in the performance of Pd/SiO2/cordierite monolith catalyst for the hydrogenation of 2-ethyl-anthraquinone. Appl Catal A: Gen 517:168

Li Y, Feng J, He Y et al (2012) Controllable synthesis, structure, and catalytic activity of highly dispersed Pd catalyst supported on whisker-modified spherical alumina. Ind Eng Chem Res 51:11083

Li Y, Feng JT, Feng YJ et al (2013) Preparation and ethylanthraquinone hydrogenation performance of Pd/Al2O3 catalyst via template-polymerization method. Chinese J Inorg Chem 29:57

Liew KH, Lee TK, Yarmo MA et al (2019) Ruthenium supported on ionically cross-linked chitosan-carrageenan hybrid MnFe2O4 catalysts for 4-nitrophenol reduction. Catalysts 9:254

Ligtenbarg AGJ, Hage R, Feringa BL (2003) Catalytic oxidations by vanadium complexes. Coord Chem Rev 237:89

Liu B, Qiao M, Deng JF et al (2001) Skeletal Ni catalyst prepared from a rapidly quenched Ni-Al alloy and its high selectivity in 2-ethylanthraquinone hydrogenation. J Catal 204:512

Liu B, Qiao M, Wang J, Fan K (2002) Highly selective amorphous Ni-Cr-B catalyst in 2-ethylanthraquinone hydrogenation to 2-ethylanthrahydroquinone. Chem Commun 2002:1236

Liu G, Duan Y, Wang Y et al (2005) Periodically operated trickle-bed reactor for EAQs hydrogenation: experiments and modeling. Chem Eng Sci 60:6270

Ma Q, Wang N, Liu G, Wang L (2019) Enhanced performance of Pd nanoparticles on SBA-15 grafted with alkyltrialkoxysilane in 2-ethyl-anthraquinone hydrogenation. Micro Mes Mat 279:245

Melada S, Rioda R, Menegazzo F et al (2006) Direct synthesis of hydrogen peroxide on zirconia-supported catalysts under mild conditions. J Catal 239:422

Niwa S, Eswaramoorthy M, Nair J et al (2002) A one-step conversion of benzene to phenol with a palladium membrane. Science 295:105

Perathoner S, Centi G (2005) Wet hydrogen peroxide catalytic oxidation (WHPCO) of organic waste in agro-food and industrial streams. Top Catal 33:207

Ranganathan S, Sieber V (2018) Recent advances in the direct synthesis of hydrogen peroxide using chemical catalysis-a review. Catalysts 8:379

Ren M, Mao M, Duan X, Song Q (2011) Hydrogen peroxide synthesis by direct photo-reduction of 2-ethylanthraquinone in aerated solutions. J Photochem Photobiol A: Chem 217:164

Ribeiro RS, Silva AMT, Figueiredo JL et al (2013) Removal of 2-nitrophenol by catalytic wet peroxide oxidation using carbon materials with different morphological and chemical properties. Appl Catal B: Environ 140:356

Ribeiro RS, Silva AMT, Figueiredo JL et al (2016) Catalytic wet peroxide oxidation: a route towards the application of hybrid magnetic carbon nanocomposites for the degradation of organic pollutants: a review. Appl Catal B: Environ 187:428

Ribeiro RS, Silva AMT, Pastrana-Martínez LM et al (2015) Graphene-based materials for the catalytic wet peroxide oxidation of highly concentrated 4-nitrophenol solutions. Catal Today 249:204

Rochefort A, Andzelm J, Russo N, Salahub DR (1990) Chemisorption and diffusion of atomic hydrogen in and on cluster models of Pd, Rh, and bimetallic PdSn, RhSn, and RhZn catalysts. J Am Chem Soc 112:8239

Rokhina EV, Virkutyte J (2010) Environmental application of catalytic processes: heterogeneous liquid phase oxidation of phenol with hydrogen peroxide. Crit Rev Environ Sci Technol 41:125

Roques J, Lacaze-Dufaure C, Mijoule C (2001) Comparison between some properties of small clusters and the (111) surface of palladium: a density-functional approach. Surf Sci 479:231

Roques J, Lacaze-Dufaure C, Mijoule C (2007) Dissociative adsorption of hydrogen and oxygen on palladium clusters: a comparison with the (111) infinite surface. J Chem Theory Comput 3:878

Rosaria C, Lorenzo A, Francesco M, Mario P (2016) Hydrogen peroxide: a key chemical for today's sustainable development. ChemSusChem 9:3374

Santacesaria E, Wilkinson P, Babini P, Carra S (1988) Hydrogenation of 2-ethyltetrahydroanthraquinone in the presence of palladium catalyst. Ind Eng Chem Res 27:780

Santacesaria E, Di Serio M, Russo A et al (1999) Kinetic and catalytic aspects in the hydrogen peroxide production via anthraquinone. Chem Eng Sci 54:2799

Santacesaria E, Di Serio M, Velotti R, Leone U (1994a) Hydrogenation of the aromatic rings of 2-ethylanthraquinone on palladium catalyst. J Mol Catal 94:37

Santacesaria E, Di Serio M, Velotti R, Leone U (1994b) Kinetics, mass transfer, and palladium catalyst deactivation in the hydrogenation step of the hydrogen peroxide synthesis via anthraquinone. Ind Eng Chem Res 33:277

Santacesaria E, Di Serio M, Velotti R, Leone U (1995) Erratum to Hydrogenation of the aromatic rings of 2-ethylanthraquinone on palladium catalyst. J Mol Catal A: Chem 99:151

Sato K, Aoki M, Noyori R (1998) A "green" route to adipic acid: direct oxidation of cyclohexenes with 30 percent hydrogen peroxide. Science 281:1646

Shaegh SAM, Nguyen NT, Ehteshami SMM, Chan SH (2012) A membraneless hydrogen peroxide fuel cell using Prussian Blue as cathode material. Energy Environ Sci 5:8225

Shang H, Zhou H, Zhu Z, Zhang W (2012) Study on the new hydrogenation catalyst and processes for hydrogen peroxide through anthraquinone route. J Ind Eng Chem 18:1851

Shen C, Wang YJ, Xu JH et al (2011) Preparation and the hydrogenation performance of novel catalyst-Pd nanoparticles loaded on glass beads with an egg–shell structure. Chem Eng J 173:226

Shi X, Yuan E, Liu G, Wang L (2016) Effects of the porous oxide layer on the performance of Pd-based monolithic catalysts for 2-ethyl-lanthraquinone hydrogenation. Chinese J Chem Eng 24:1570

Sun YS, Wang YJ, Lv YC et al (2008b) Subcritical water treatment: a simple method to prepare porous glass with a core–shell structure. J Am Ceram Soc 91:103

Sun YS, Wang YJ, Lv YC, Luo GS (2008a) Heavy metal ion sorption properties of porous glass beads with a core-shell structure. SolvExtr Ion Exch 26:672

Surisetty VR, Dalai AK, Kozinski J (2010) Intrinsic reaction kinetics of higher alcohol synthesis from synthesis gas over a sulfided alkali-promoted Co–Rh–Mo trimetallic catalyst supported on multiwalled carbon nanotubes (MWCNTs). Energy Fuels 24:4130–4137

Tan J, Zhang J, Lu Y et al (2012) Process intensification of catalytic hydrogenation of ethylanthraquinone with gas-liquid microdispersion. AIChE J 58:1326

Tanev PT, Pinnavaia TJ (1996) Biomimetic templating of porous lamellar silicas by vesicular surfactant assemblies. Science 271:1267

Tang P, Chai Y, Feng J et al (2014) Highly dispersed Pd catalyst for anthraquinone hydrogenation supported on alumina derived from a pseudo-boehmite precursor. Appl Catal A: Gen 469:312

Toshima N, Ito R, Matsushita T, Shiraishi Y (2007) Trimetallic nanoparticles having a Au-core structure. Catal Today 122:239–244

Ulmann T (1994) Encyclopedia of industrial chemistry. VCH, Vol. A13,Weinheim, pp. 443-466

Van Oss JF (1968) Chemical technology. Vol. 1, Barnes and Nobel Inc. New York, pp. 195-201

Vieira Y, Ceretta MB, Foletto EL et al (2020a) Application of a novel rGO-CuFeS$_2$ composite catalyst conjugated to microwave irradiation for ultra-fast real textile wastewater treatment. 36:1010397.

Vieira Y, Martinello KDB, Ribeiro TH et al (2022) Photo-assisted degradation of organic pollutant by CuFeS2 powder in RGB-LED reactors: a comprehensive study of band gap values and the relation between wavelength and electron-hole recombination. Adv Powder Techn 33:103368

Vieira Y, Silvestri S, Leichtweis J et al (2020b) New insights into the mechanism of heterogeneous activation of nano–magnetite by microwave irradiation for use as Fenton catalyst. J Environ Chem Eng 8:103787

Xu L, Zhao H, Song H, Chou L (2012) Ordered mesoporous alumina supported nickel-based catalysts for carbon dioxide reforming of methane. Int J Hydrogen Energy 37:7497

Yamada Y, Yoneda M, Fukuzumi S (2013) A robust one-compartment fuel cell with a polynuclear cyanide complex as a cathode for utilizing H$_2$O$_2$ as a sustainable fuel at ambient conditions. Chem Eur J 19:11733

Yamazaki SI, Siroma Z, Senoh H et al (2008) A fuel cell with selective electrocatalysts using hydrogen peroxide as both an electron acceptor and a fuel. J Power Sour 178:20

Yang F, Cheng K, Wu T et al (2013) Preparation of Au nanodendrites supported on carbon fiber cloth and its catalytic performance to H_2O_2 electroreduction and electrooxidation. RSC Adv 3:5483

Yang X, Chen D, Liao S et al (2012) High performance Pd-Au bimetallic catalyst with mesoporous silica nanoparticles as support and its catalysis of cinnamaldehyde hydrogenation. J Catal 291:36

Yao H, Shen C, Wang Y, Luo G (2016a) Catalytic hydrogenation of 2-ethylanthraquinone using an in situ synthesized Pd catalyst. RSC Adv 6:23942

Yao Y, Wu G, Lu F et al (2016b) Enhanced photo-Fenton-like process over Z-scheme $CoFe_2O_4$/g-C_3N_4 heterostructures under natural indoor light. Environ Sci Pollut Res 23:21833

Yuan E, Wu C, Hou X et al (2017) Synergistic effects of second metals on the performance of (Co, Ag, Cu)-doped Pd/Al_2O_3 catalysts for 2-ethyl-anthraquinone hydrogenation. J Catal 347:79

Yuan E, Wu C, Liu G, Wang L (2016) One-pot synthesis of Pd nanoparticles on ordered mesoporous Al_2O_3 for catalytic hydrogenation of 2-ethyl-anthraquinone. App Catal A: Gen 525:119

Zhang J, Gao K, Wang S et al (2017) Performance of bimetallic PdRu catalysts supported on gamma alumina for 2-ethylanthraquinone hydrogenation. RSC Adv 7:6447

Zhang J, Li D, Zhao Y et al (2008) A Pd/Al_2O_3/cordierite monolithic catalyst for hydrogenation of 2-ethylanthraquinone. Catal Commun 9:2565

Zhang Q, Li J, Liu X, Zhu Q (2000) Synergetic effect of Pd and Ag dispersed on Al_2O_3 in the selective hydrogenation of acetylene. Appl Catal A: Gen 197:221

Zhou C, Lai C, Huang D et al (2018) Highly porous carbon nitride by supramolecular preassembly of monomers for photocatalytic removal of sulfamethazine under visible light driven. Appl Catal B: Environ 220:202

Zhou WP, Lewera A, Larsen R et al (2006) Size effects in electronic and catalytic properties of unsupported palladium nanoparticles in electrooxidation of formic acid. J Phys. Chem B 110:13393

Zudin VV, Likholobov VA, Yermakov YI (1979) Catalytic synthesis of hydrogen peroxide from oxygen and water in the presence of carbon monoxide and phosphine complexes of palladium. Kinet Catal 20:1559